CHAPTER III
ELECTRICAL & OPTICAL PROPERTIES OF As_2S_3 THIN FILMS

CHAPTER III

ELECTRICAL AND OPTICAL PROPERTIES OF As_2S_3 THIN FILMS

3.1 Introduction

The experimental details necessary for deposition of the arsenic trisulphide thin films are presented in chapter II. Our aim is to prepare arsenic trisulphide thin films by a chemical deposition method and to study its electrical and optical properties indetail. It is therefore essential to characterise the As_2S_3 thin films for their electrical, optical and structural properties. This chapter is devoted partly to the necessary design/fabrications and experimental techniques that were used for the electrical and optical properties and partly for the measurement of layer thickness, optical and electrical characterisations. The optical and electrical characterisation involve measurements of electrical conductivity, thermoelectric power, optical absorption, and calculation of the carrier concentration, mobility, grain barrier height, absorption coefficient , optical band gap etc.

3.2 Experimental Details

Details of the preparation procedure and mechanism of film formation for arsenic trisulphide thin layers are given in sections 2.3.4 and 2.3.5, respectively. The method involves: a reaction container consisting of a clear methanolic solutions of 0.5M arsenic trichloride and 0.5 M thiourea in their 2:3 volumetric ratio. The substrates were attached to a specially designed substrate holder and were assembled in a reaction mixture. The deposition was allowed for up to 120 hour and the substrates were taken out one by one from the reaction bath after every 12 hour deposition time. The deposition of As_2S_3 thin films was also carried out at 40°C, 55°C and 70°C in order to

understand role of the deposition temperature on the growth mechanism.

3.2.1 Thickness measurement

The layer thickness measurement was carried out by using a weight-difference-density method. The mass, area and density of the material were considered in this method. The film layer thickness is related to the mass, area and density as;

$$t = \frac{m}{A.d} \qquad \ldots(3.1)$$

where,

m = weight of the sample in gm

A = sample area in cm^2

d = density of the material in $gm\text{-}cm^{-3}$.

3.2.2 Design of conductivity measuring unit and measurement of conductivity

The dc electrical conductivity of the sample in dark was measured by using a two probe conductivity measuring unit designed and fabricated in our laboratory. The unit is shown in Fig. 3.1 and it consists of two brass plates of the dimension 10 cm x 5 cm x 0.6 cm fitted one over the other. The lower plate is fitted tightly on a asbestos base of the dimension 10 inches x 10 inches. Two strip heaters (65 W) were kept in parallel on the lower brass plate and the other plate was fixed tightly to the lower plate so as to achieve make sandwich of the heaters between the two brass plates. A thick multilayered mica sheet was used to wrap the heaters before being put in between the brass plates so as to achieve the electrical insulation from either of the brass

Fig. 3.1

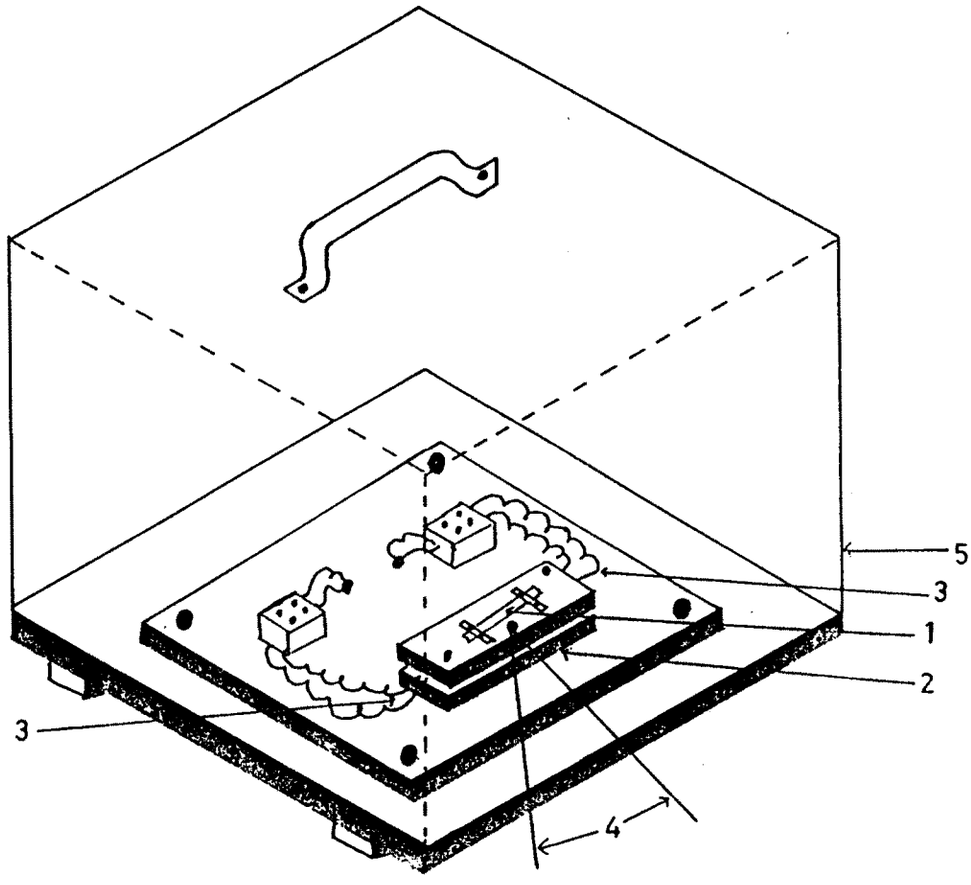

Fig. 3.1 Design and experimental arrangement for the measurement of conductivity
1) Sample, 2) Brass plates, 3) Electrical heaters, 4) Thermocouple, 5) Shield.

plates. An aluminium sample holder of the dimensions 3 cm x 0.5 cm x 0.6 cm was designed, fabricated and fixed exactly at the centre of the upper plate. A sample whose conductivity was to be measured was mounted with a copper point press contacts below the sample holder. The area under consideration was defined with the rest sample erased. The sample was electrically insulated from the upper brass plate and the sample holder by interposing the micapieces at the appropriate places. Thermal radiation losses were reduced by covering whole the set up in a bakelite box. The box was coated by means of asbestos sheets from inside. The working temperature was recorded with a Chromel-Alumel thermocouple(24 guage) fitted at the centre on the top of the upper brass plate. A regulated power supply unit was used to pass the current through the sample. A fixed potential drop was applied across the sample and the current was noted for various working temperatures. The current through the sample was measured using a FET input 4 1/2 digit nanoammeter, DNM-121,(Scientific Equipments Roorkee). A photograph showing an experimental set up is shown in the Fig.3.2.

3.2.3 Design of thermoelectric power unit and measurement of thermoelectric power

Bauerie et al/1/ have pointed out the knowhow for measurement of the thermoelectric power. The maximum temperature difference and minimum contact resistance are the major requirements. The thermoelectric power unit was fabricated considering the above two requirements. Fig.3.3 shows a schematic of the thermoelectric power measurement unit consisting of two

Fig. 3.2

Fig. 3.2 Photograph of Conductivity measuring set-up

1. microvoltmeter
2. powerr supply
3. current meter
4. conductivity unit

Fig. 3.3

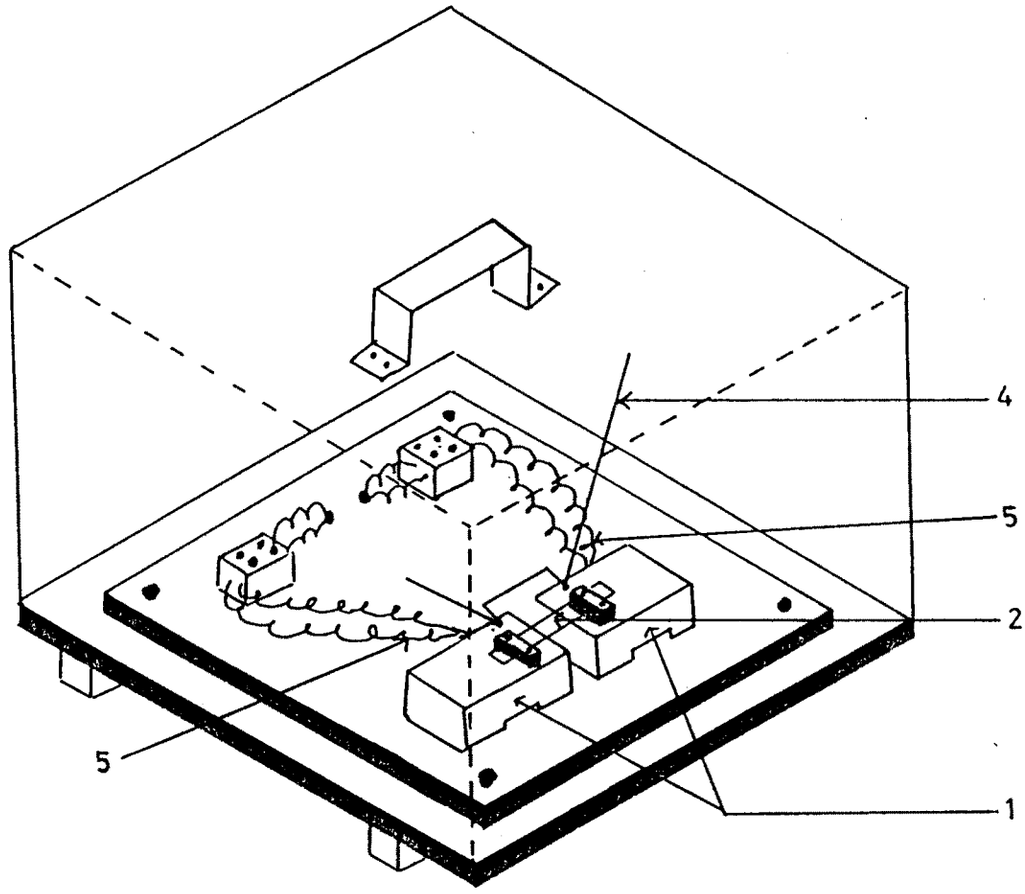

Fig. 3.3 Design and experimental arrangement for the measurement of TEP
1) Copper blocks, 2) Sample
3) Thermocouple (mean temperature recorder),
4) Differential thermocouple (thermo - voltage recorder), 5) Heaters.

brass plates of the dimensions 5 cm x 4 cm x 1.2 cm fitted on a asbestos sheet supported by a bakelite sheet. The plates were arranged in parallel separated by a distance of 3cm. They were pitched from the bottom to a size of the miniheater and miniheaters of the different wattages (65 W and 35 W) were fixed in them. The electrical insulation between the miniheaters and the brass plates was achieved by means of mica sheets. A pair of sample holder, fabricated in a similar fashion as that of the conductivity measurement technique was fitted on the top adjacent near edges of the brass blocks lengthwise. The sample size used in this measurement was 3.5 cm x 0.5 cm on amorphous glass substrate. The dimensions of the substrate holder were 3 cm x 0.5 cm x 0.6 cm. The sample was also electrically insulated from the brass blocks and the substrate holder by means of mica pieces. The press point copper contacts were used for the measurement. The Chromel-Alumel thermocouple (24 gauge) was fixed on the top of the brass blocks for the temperature measurement. The unit was properly shielded by a bakelite box to minimise the losses due to the thermal radiations. The thermovoltage generated by a sample was measured by a H.P.-3441, 4 1/2 digit microvoltmeter. The temperature gradient was measured with an HIL- 2665, 4 1/2 digit microvoltmeter.

3.2.4. Optical absorption measurements

The estimation of the optical energy gap and absorption coefficient were done from these measurements. The type of optical transitions was also determined from these studies. Actually the measurements were performed to determine the

optical density as a function of the wavelength. A Shimadzu 160A-UV-Visible Spectrophotometer was used for this purpose. The range of wavelength used was from 3000A° to 8000A°.

3.3 Results and Discussion

3.3.1 Physical observations

The arsenic trisulphide thin film layers were obtained onto the ordinary glass substrates by a chemical bath deposition method. The actual preparation was carried out in an acidic medium in the presence of methanol as the reducing agent. The film formation was therefore made possible on the basis of the slow release of As^{+3} and S^{2-} ions and subsequent condensation on the substrate support/5,6/. It appeared from the growth mechanism that the rate of film formation would increase with increasing the concentration of As^{+3} and S^{2-} ions and hence chemical compositions were varied randomly to obtain good quality films and to optimise the preparative conditions. It is only the appearance and physical properties of the samples from which we have, for the present case, decided the quality of the samples. The deposition time and temperature required to produce relatively better samples were also fixed. For our experimental conditions and at a working temperature (optimised) equal to 27°C and deposition time of 96h; highly uniform, crackfree, strongly adherent, smooth and diffusely reflecting arsenic trisulphide films with a terminal thicknes around 0.4 to 0.5 μm have been obtained. An increase in deposition temperature reduces the deposition time down to 12h. The comparison of both samples showed that an increase in deposition temperature yields samples

to be of the poor quality. Secondly, the deposits were flaky, less adherent, powdery and non-uniform in nature. Therefore, we have preferred the sample deposition at room temperature. The as-deposited layers are pale yellow in color and baking around 200°C results into dark orange red color of the samples. For intermediate baking temperatures, the sample color appeared to be a mixture of both yellow and orange-red colors. Fig.3.4 shows growth kinetics for the films grown on the glass surface. It is seen that, at room temperature, the growth rate of the film in the early stages of the film growth is with deposition time almost linearly and it then decreases to, a negligible value showing saturation in the terminal thickness of a layer. The enhancement in growth rate was then observed for two typical temperatures (40°C and 55°C). For higher temperatures, the growth rate is initially high and this may be explained on the basis of the higher rate of release of the As^{3+} and S^{2-} ions in the solution as is the case for cadmium sulphide thin films /7-10/. Moreover, the higher rate of release of ions causes an increased amount of interraction between the ions and the volume nucleation centres on the substrates that results into the subsequent condensation of the ions on the substrates/6,9/. Obviously the process would reduce the deposition time. In our case, a deposition temperature of 55°C, reduces the deposition time down to 18hours/9-10/. It is also observed that, the terminal thickness is reduced. The reason is that, at high temperature, the rate of reaction tends towards precipitation rather than the film formation/9-10/. Further, it is probable that not all the ions that are released as a result of high temperature may get

Fig3.4

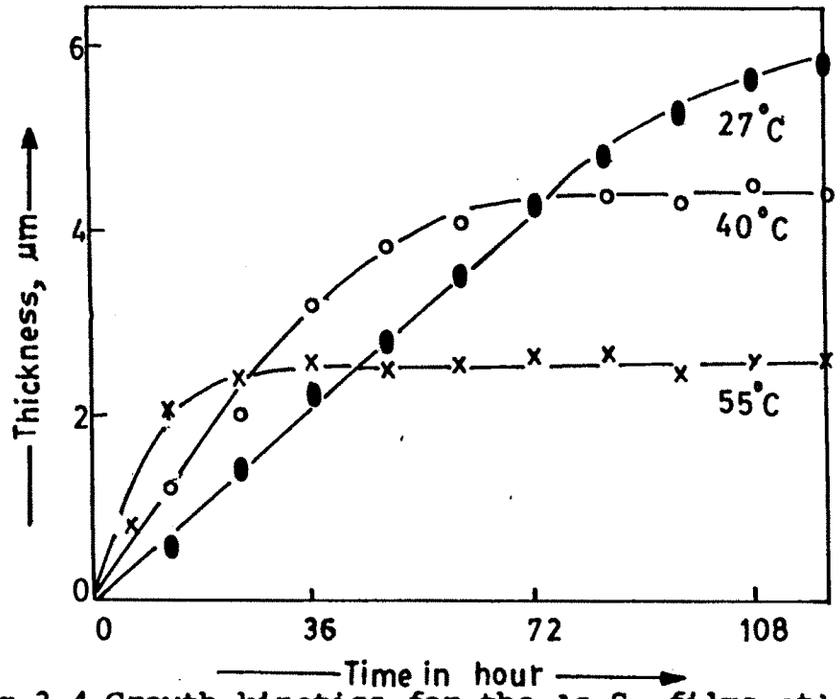

Fig.3.4 Growth kinetics for the As_2S_3 films at: I)●-27°C, II)○-40°C III)×- 55°C

Fig.3.5

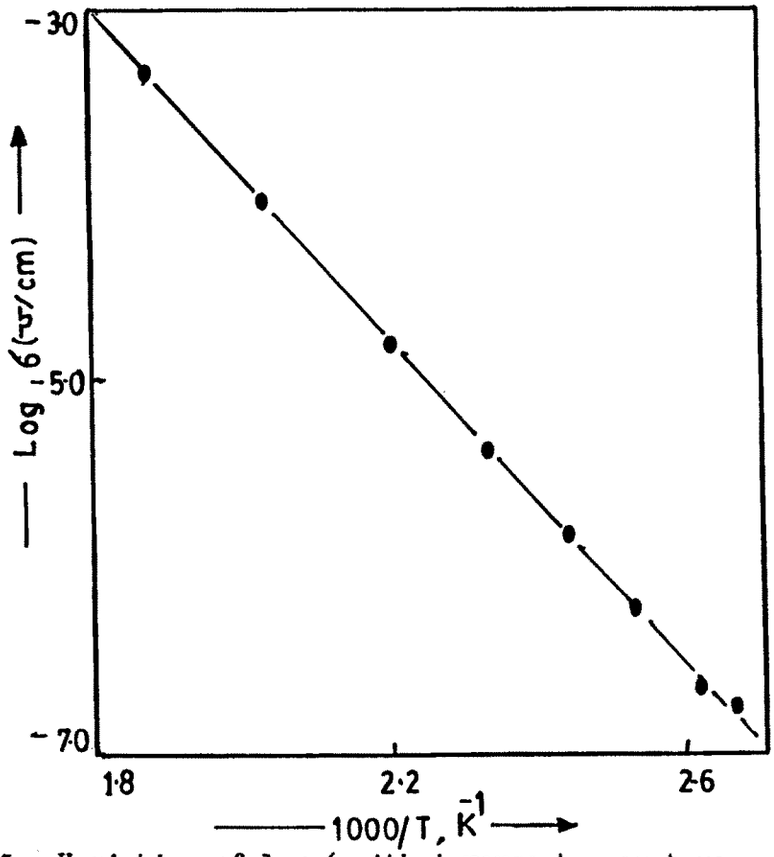

Fig. 3.5 Variation of log 6 with inverse temperature for the As_2S_3 films

sufficient time to condense on the substrate surface. This resulted in decreased thickness of a layer/9,10/.

3.3.2 Electrical properties

a) Electrical conductivity

The electrical resistance of the sample, in dark, was measured in the temperature range from 300 to 575 K for both heating and cooling cycles. The electrical resistance decreases with the increase in temperature indicating the semiconducting nature of the sample. At room temperature As_2S_3 has a typical value of electrical conductivity equal to 10^{-9} ohm-cm^{-1}. It is also found that a plot of logR vs 1/T is linear and gives the thermal energy gap (E_{gth})in the intrinsic region of the semiconductor. The temperature variation of logarithm of conductivity is shown in Fig.3.5.

It is seen that both for heating and cooling cycles the variation of log σ vs 1/T follows approximately the same track which partly confirms the uniformity of the samples those are deposited using our chemical bath deposition process. The temperature variation of an electrical conductivity can be expreseed by usual Arrhenius relation;

$$\sigma = \sigma_o \exp(-Ea\sigma /kT) \qquad ...(3.1)$$

where, Eaσ is the conductivity activation energy, in eV, T is the absolute temperature in K and k is the Boltzmann's constant. The conductivity activation energy is calculated from the slope of the linear region of the log σ vs 1/T variation and is found to be 0.837 eV. The magnitude of Eaσ is found to be smaller than

those reported earlier. This can be attributed to the comparitively lower resistivity of our samples than the samples prepared by other conventional techniques viz. solution gas interface technique, dip and dry, spray pyrolysis, vacuum evaporation, sintering, sulfurization etc. The lower resistivity observed in our case can be due to the improved degree of crystallinity provided by the preferred orientation during growth process.

At high temperature (>450 K) fast increase in conductivity is observed which can be attributed to the fact that at high temperature, jumping of electrons from one arsenic site to other take place/12/. It is reported that when bands are narrow with the presence of localised states, the conduction occurs due to hopping mechanism/12/. The activation energy can then be considered to be the energy required for hopping/12/.

b) Thermoelectric power

Another method to characterize the semiconducting materials is the thermoelectric power measurement technique. This involves measurement of thermally generated voltage of a sample. The technique also helps to detect the type of conductivity of the material under investigation. The thermoelectric power (P) generated by a As_2S_3 sample was measured in the temperature range from 300 K to 450 K and the sample is found to be of the n-type conduction. The order of the generated thermovoltage is uV. The temperature dependence of thermoelectric power is shown in Fig.3.6. The thermoelectric power (P) varies with temperature (T) according to the relation /13,14,15/;

Fig. 3.6

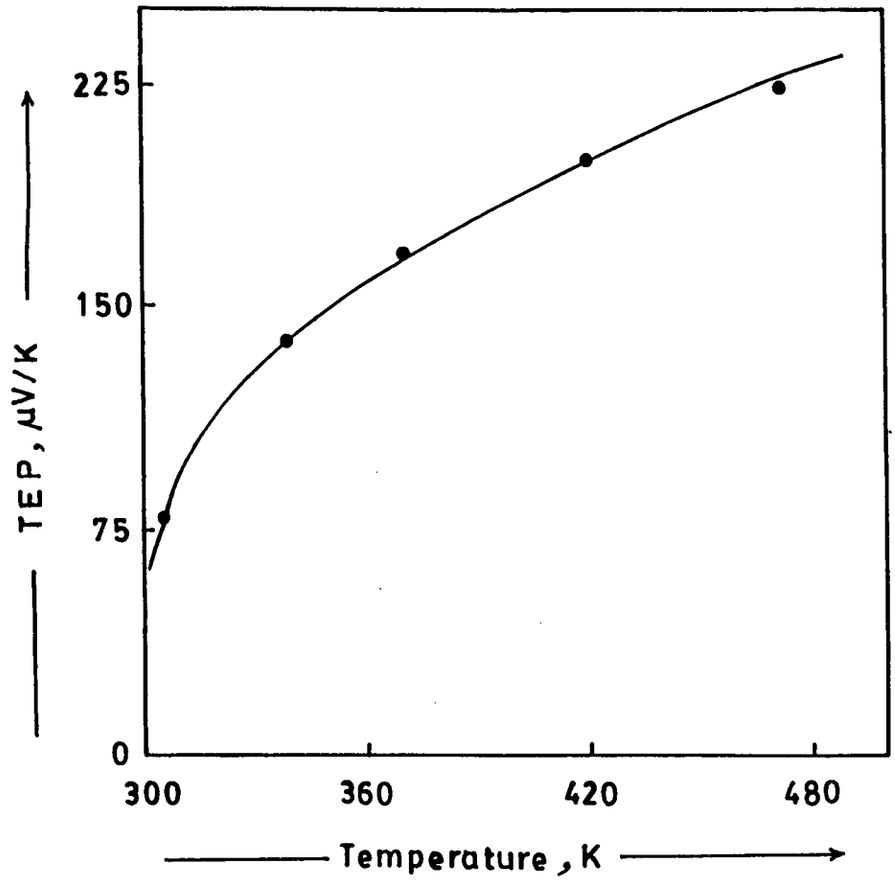

Fig. 3.6 Variation of thermoelectric power with working temperature for a typical As_2S_3 sample.

$$P = -\frac{k}{q}\left(A + \ln \frac{2(2m_e^{*}\, kT)^{3/2}}{nh^3} \right) \qquad \ldots(3.2)$$

where, q is an electronic charge, h is Planck's constant, A is the thermoelectric factor introduced by the kinetic energy of electrons and hence depends on the scattering process, n is the carrier concentration, m_e^{*} is the effective mass of an electron, k is the Boltzmann's constant and T is the absolute temperature.The thermoelectric power is observed to increase with increase in temperature. The conductivity and thermoelectric power data are used to calculate the carrier density. The room temperature magnitude of carrier concentration is 10^{17} cm^{-3}. The temperature dependance of carrier concentration is shown in Fig.3.7. The carrier mobilities at different temperatures are determined by using standard relation;

$$\mu = \frac{\sigma}{ne} \qquad \ldots (3.3)$$

Fig.3.8 shows sketch of carrier mobility as a function of temperature. It is interesting to note that the carrier density is somewhat weak function of working temperature, however, changes in carrier mobility are significant. The increasing dependance of carrier mobility on temperature suggests the possibility of scattering mechanism associated with the intergrain barrier. The temperature dependant grain boundary mobility is related to the grain boundary potential as;

$$\mu = \mu_o \exp(- \Phi_B / kT) \qquad \ldots(3.4)$$

Fig. 3.7

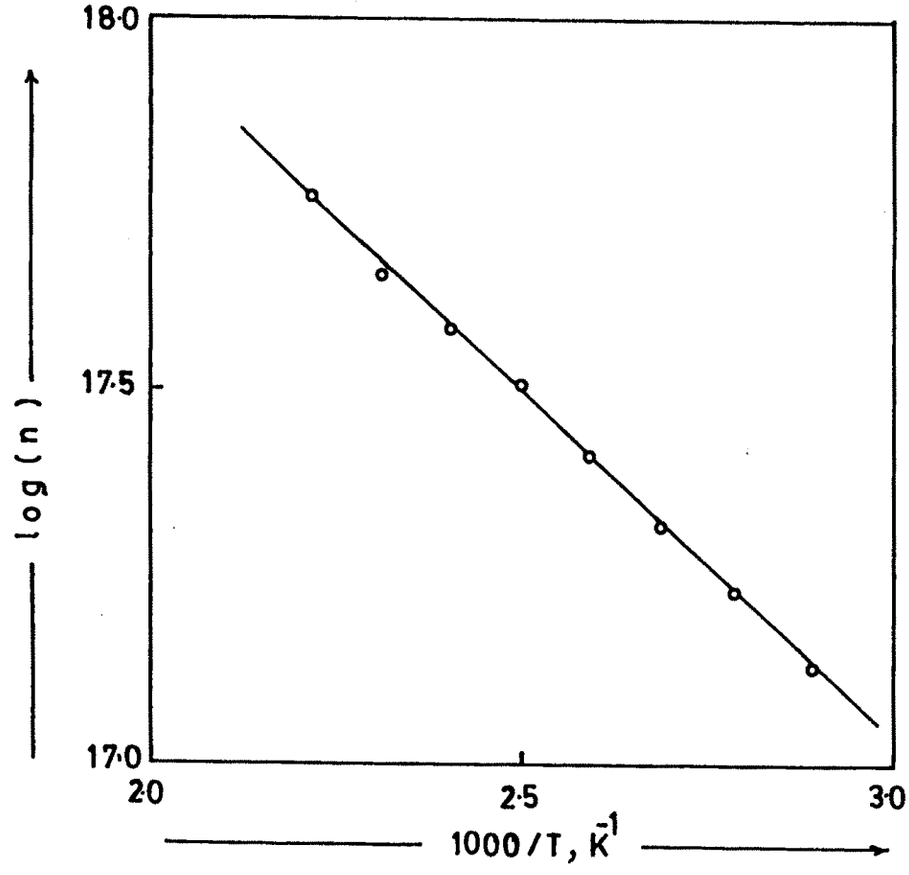

Fig. 3.7 Variation of carrier concentration (n) with inverse of the temperature.

Fig.3.8

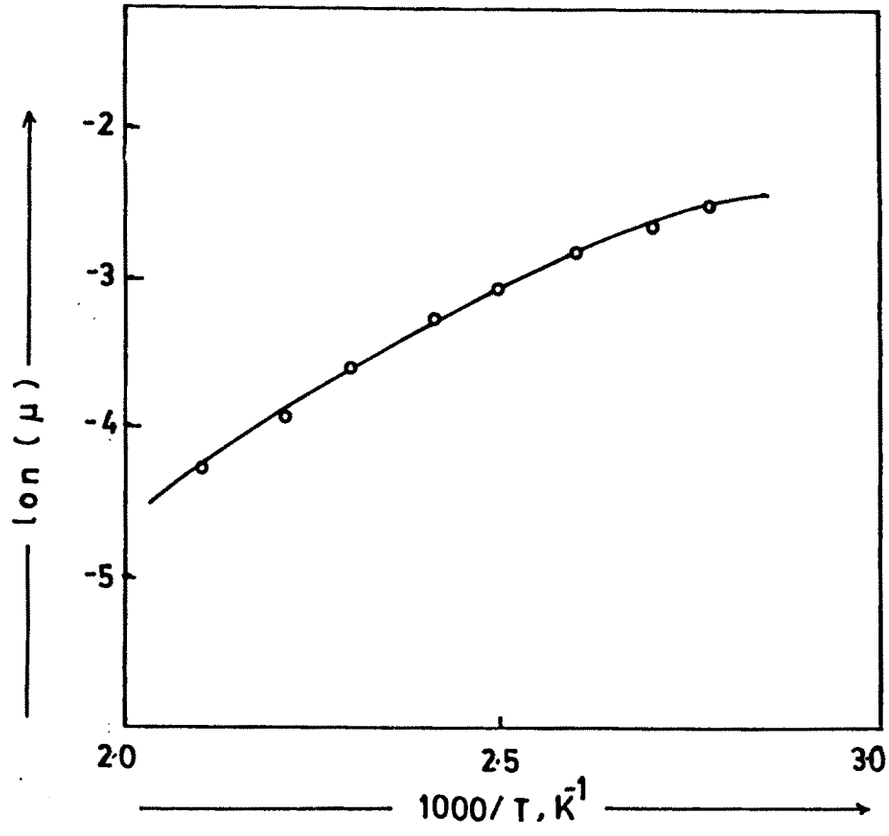

Fig. 3.8 Variation of carrier mobility (μ) with inverse of the temperature.

where, Φ_B is the height of the potential barrier at the grain boundary, and u_o is the preexponential factor which, on the assumption that the current over the barrier flows by thermionic emission, depends on the grain size (d) and the effective mass of an electron (m^*) as;

$$\mu_o = (e.d / 2 \pi m^* kT)^{1/2} \qquad ...(3.5)$$

The grain barrier height (Φ_B) is then determined from the $\ln(\mu T^{1/2})$ vs 1/T plot and is shown in Fig.3.9. The observed grain barrier height (Φ_B) is 0.638 eV. It should be noted that the sum;

$$E_{an} + \Phi_B \simeq E_{a\sigma} \qquad ...(3.6)$$

which should be expected from the interrelationship of conductivity, carrier density and mobility. In our case it is seen that the relation (3.6) hold good. The results are in close agreement with those reported earlier/12,16,17/.

3.3.3. Optical properties

Studies on optical and structural aspects of V-VI chalcogenides have been chiefly restricted to the sputtered and vacuum evaporated thin films/18,19/. However, flash evaporation, chemical transport, dip- dry, solution gas interface technique and solution growth (or chemical deposition) could be used to obtain homogeneous thin films /19,20,21/. The literature survey points out that the conventional solution growth technique is being widely employed for the growth of binary and ternery compounds. If the experimental results on optical studies are to be interpreted properly, it is important to know the type of

Fig. 3.9

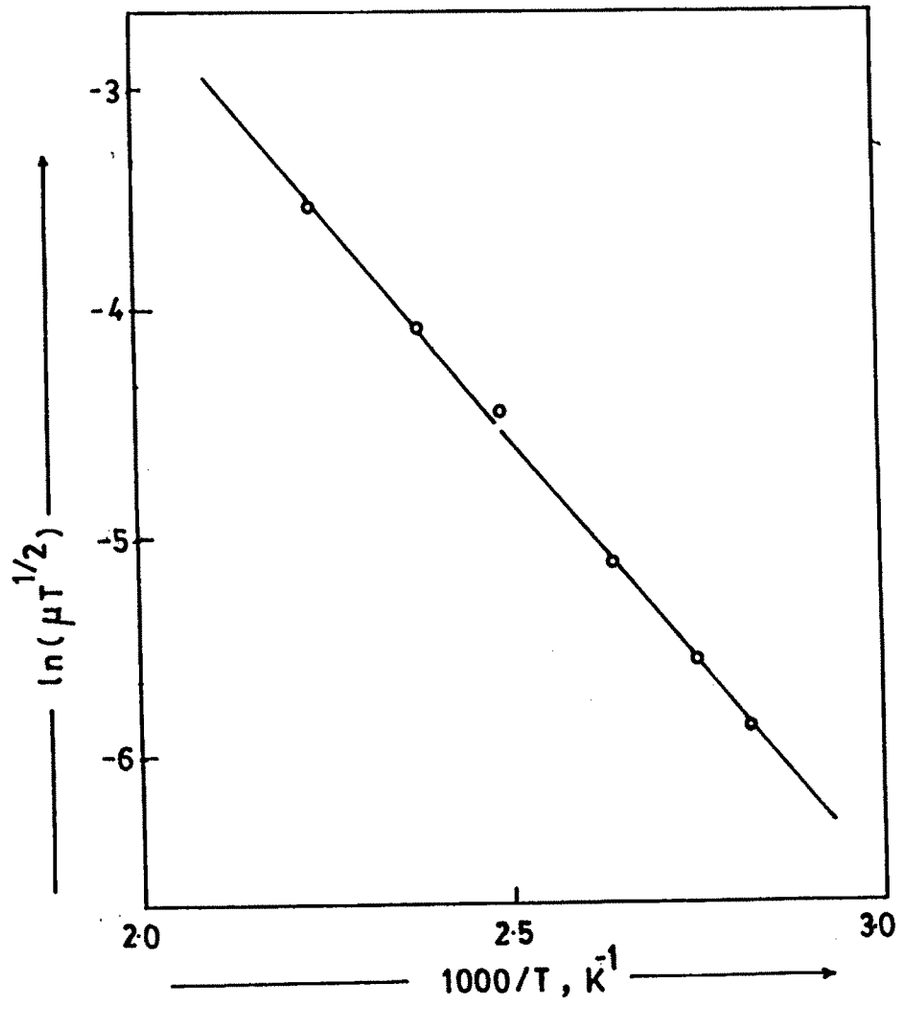

Fig. 3.9 Determination of intercrystalline barrier height (Φ_B) from $\ln\mu T^{1/2}$ vs $1/T$ plot for the As_2S_3 film.

transitions that are taking place in the material under investigation. It is also possible to differentiate direct and indirect type of transitions by examining the energy ($h\nu$) dependence of the absorption coefficient (α). Therefore, the As_2S_3 thin films have been further characterised by means of an optical technique. The optical absorption spectrum for As_2S_3 thin layer is obtained at 300K in the 3000 A° - 8000 A° wavelength range.

The absorption coefficient is high and is of the order of 10^{+4}-10^{+5} cm^{-1}. The energy absorption spectrum is shown in Fig.3.10. The absorption spectra for as-deposited and heat treated samples have been studied at room temperature without accounting for reflection and transmission losses. The spectra showed clearly the absorption edge at 525 nm for as-deposited sample and the absorption edge shifts towards higher energy side for heat treated samples. The data have been analysed from the following classical relation for near edge optical absorption in semiconductors;

$$\alpha = \frac{K\,(h\nu - Eg)^{n/2}}{h\nu} \qquad \ldots(3.7)$$

where, K is the constant, Eg is the separation between the valence and conduction bands, n is a constant unity for direct gap semiconductors while four for an indirect gap materials. The variation of $(\alpha h\nu)^2$ vs $h\nu$ is linear and is shown in Fig.3.11, which means that the mode of transition in As_2S_3 films is of the direct type. Extrapolation of these curves on energy axis gives

Fig. 3.10

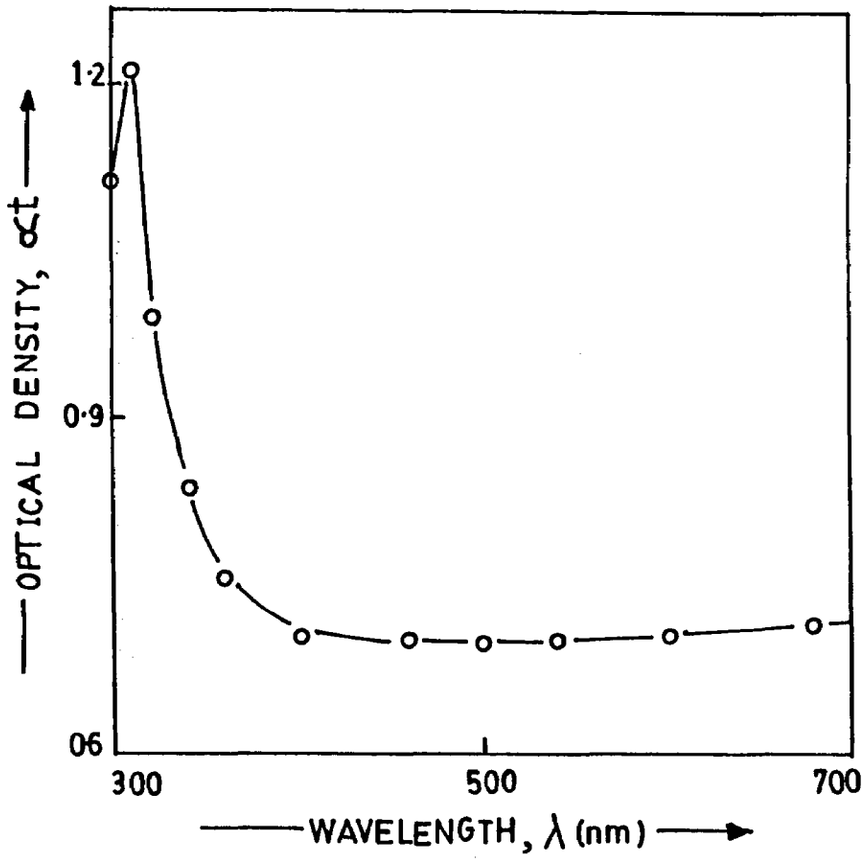

Fig. 3.10 Variation of an optical density with the incident wavelength (λ) for As_2S_3 thin film.

Fig. 3.11

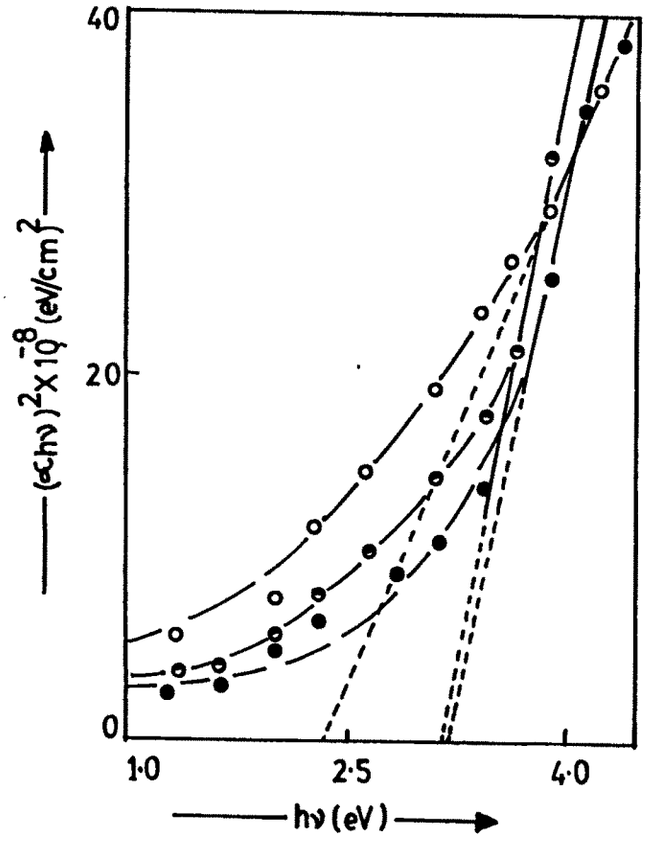

Fig. 3.11 Determination of the energy gap for the As_2S_3 samples.
1. O-as deposited, 2. ● -200°C and
3. ⊖ - 250°C

the optical energy gap (Eg) equal to 2.35 eV for untreated sample which is in close agreement with the previous reports/22,23,24/ while 3.2 eV and 3.15 eV for the samples baked at 200°C and 250°C respectively. It is seen that the band gap is increased after heat treatment, a typical unusual observation compared with the other semiconductors in which bandgap decreases after heat treatment/7,10/. In our case the increase in band gap can be related to the glassy structural changes that are observed above the transition temperature /9,10,25/. This has also been confirmed from the XRD and SEM observations as indicated in chapter IV. The appearance of an exponential tail within the same energy range is a characteristic of chalcogenides microcrystalline materials /9,10,13/. Mode of optical transitions is also examined for this material by the variation of α^2 vs $h\nu$ as suggested by Shanti et al /26/. It is found that the variation is straight line showing direct type of transition. The variation is depicted in Fig. 3.12.

3.4 Conclusions

A novel and easiest way of obtaining As_2S_3 thin films using a chemical growth process is presented. The deposition is carried out in an acidic medium and growth of the thin film is by slow release of As^{3+} and S^{2-} ions in a complex solution and subsequent condensation on the substrate support. Good quality depostion of As_2S_3 thin films with less consumption of both the electrical power and active materials is possible. The as-deposited samples are pale yellow in colour and the colour changes through dark yellow and finally faint-orange red above 200°C. The samples are

highly resistive with n-type conduction. An activation energy of electrical conduction is 0.837 eV and the thermally generated voltage is of the order of microvolts. The data on optical studies show high absorption coefficient (10^{+4} - 10^{+5} cm^{-1}), direct mode of transition and forbidden energy gap of 2.35 eV for as-deposited sample while 3.2 eV and 3.15 eV for the samples baked at 200°C and 250°C respectively.

Fig. 3.12

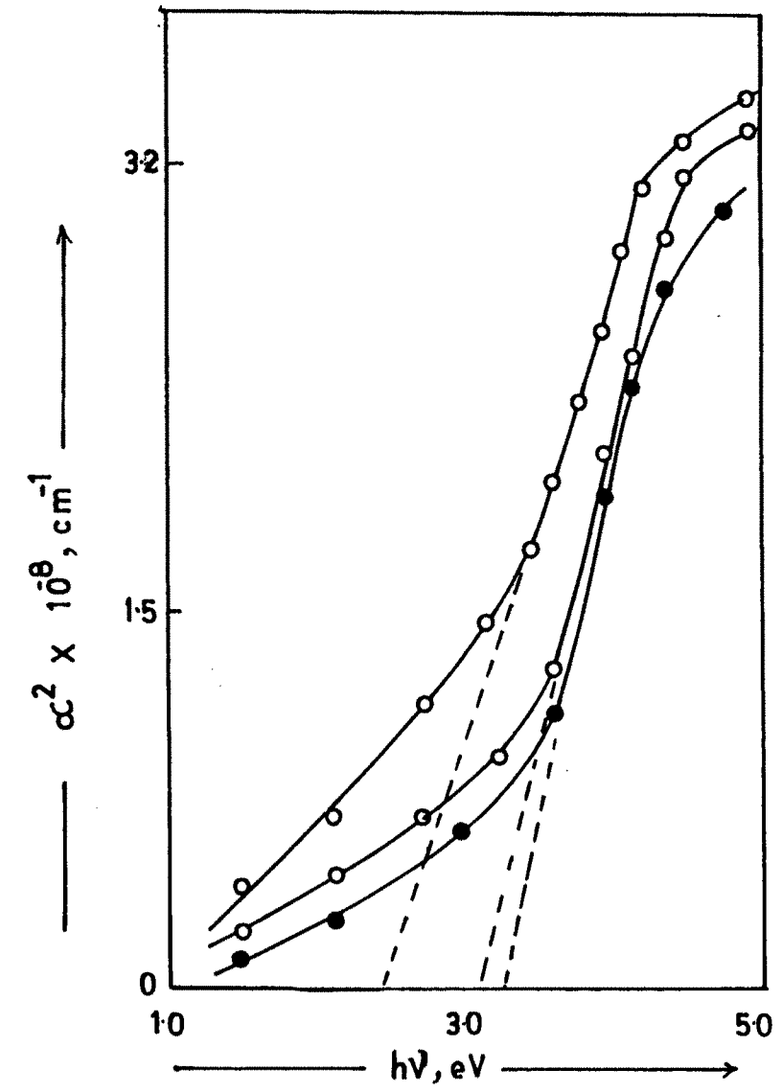

Fig. 3.12 Variation of α^2 vs $h\nu$ for the As_2S_3 thin film.
i) o- as deposited, ii) ●- 200°C and iii) ⊖- 250°C

References

1. J.E.Bauerie, P.H. Sutter and R.W.Ure, in "Thermoelectricity" Science and Technology, (eds) R.R. Heikel and R.W.Ure, Interscience Publishers, (1969)p.285.
2. Gracia, J. G., Martinez-Montes and R. S. Gonzalez, J. Electrochem. Soc,139(1992).
3. C. V. Surynarayana, A.S. Lakshmanan, V. Subramanian and R. Krishnakumar Bull. Electrochem. 2(1986)57.
4. T.L.Chu, S.S.Chu, N. Schultz, C. Wang and C.Q. Wu J., Electrochem. Soc, 139(1992)2443.
5. I. Kaur, D.K. Pandya and K.L. Chopra, J. Electrochem. Soc; 127(1980)943.
6. O.Savadogo and K.C. Mondal, Sol.Eng.Mat. & Solar Cells; 26(1992)117.
7. A. Mondal and P. Pramanik, J. Solid State Chem; 47(1983)81.
8. R.C. Kainthla, D.K. Pandya and K.L.Chopra, J. Electrochem. Soc; 127(1980)277.
9. L. P. Deshmukh, J. S. Dargad & C. B. Rotti Ind. J. Pure and Appl. Phys; 33(1995) 687.
10. L. P. Deshmukh, J.S. Dargad, C. B. Rotti, S.G.Holikatti, G.S. Shahane, K. M. Garadkar and P. P. Hankare, Proc. Nat. Conf. On Thin Film Processing and its Applications, 22-24 Jan. 1995, S. V. University, Tirupati (A.P.), (India).
11. L.P. Deshmukh, S.G. Holikatti, B.P. Rane, B. M. More and P. P. Hankare, J. Electrochem. Soc., 141(1994)1779.
12. B. Roy, B. R. Chakraborthy, R. Bhattacharya and A. K. Dutta, Solid State Commun., 25(1978)937.

13. S. H. Pawar, P. N. Bhosale and M. D. Uplane, Ind. J. Pure and Appl. Phys., 21(1983)665.
14. Y. Y. Ma and R. H. Buhe, J. Electrochem. Soc., 124(1977)1430.
15. L. P. Deshmukh, V. S. Sawant and A. B. Palwe, Sol. Energ. Mat., 20(1990)341.
16. P. N. Bhosale, Ph. D. Thesis, Shivaji University, Kolhapur, (1985), M. S.(India).
17. S.H.Pawar, in "Studies on large area Semiconductor Liquid Junction Photovoltaic Cells", DNES Project no.:(1)/3/8/NEs/448,(1985).
18. C. W. Moulton, Nature, 196(1962)793.
19. P. A. K. Moorthy, J. Mat. Sci. Lett.,3(1984)55.
20. B.B. Nayak, H. N. Acharya, T. K. Choudhari and G. B. Mitra, Thin Solid Films.,92(1982)309.
21. P. Pramanik and R. N. Bhattacharya, J. Electrochem. Soc., 127(1980)2087.
22. E. Hajto, P.J.S. Ewan, R. Belford et al, J. Non. Crys. Solids, 97-98(1987)1191.
23. B. T. Kolomiets, T. N. Mamonotova and V. V. Negreshul, Phys. Status Solidi(a), 27(1968)1.
24. G. Ghosh and B. P. Verma, Thin Solid Films, 60(1979)61.
25. K. White, B. Kumar and A. K. Rai, Thin Solid Films, 161(1988)139.
26. E. Shanthi, V. Dutta, A. Banerjee and K.L. Chopra, J Appl. Phys., 51(1980) 6243.